CrossMark

PEER REVIEWED

Characterizations of Composite Titanium Nitride Coatings Deposited by Very Low-Pressure Plasma Spraying

Xiujuan Fan[1] · Geoffrey Darut[1] · Marie-Pierre Planche[1] · Xiaohua Feng[2] · Hanlin Liao[1] · Ghislain Montavon[1]

Abstract In this study, composite titanium nitride coating deposition by reactive spraying was carried under a controlled low-pressure (150 pa) atmosphere with a F4-VB low-power plasma gun. Pure titanium powder is injected into the plasma, and a reactive gas (N_2) is added on the substrate surface to generate nitriding reactions. The experiments were carried out at different radial distances of the plasma plume. Morphologies of the coating present quite dense binary structure deposited by molten, vapors particles. As measured by means of x-ray diffraction, the coatings composition is modified with an evolution of $TiN_{0.3}$, Ti_2N and TiN phase crystalline phases along radial distance of the plume. The nitride phases (Ti_2N, TiN) contents of the coating show a linear relationship with the micro-hardness of the coating. Micro-hardness of VLPPS-processed composite titanium coatings reaches $1071HV_{0.03}$.

✉ Xiujuan Fan
   xiujuan.fan@utbm.fr

1 ICB, UMR 6303, CNRS, Univ. Bourgogne Franche-Comté, UTBM, 90010 Belfort, France

2 Ningbo Institute of Materials Technology and Engineering, Chinese Academy of Sciences, Ningbo 315201, People's Republic of China

Introduction

TiN ceramics draw the attention of people due to their good mechanical properties, high thermal resistance, excellent chemical stability and biocompatibility (Ref 1-3). TiN layers have a wide potential of applications in aerospace, marine and biomedical areas, etc. (Ref 4, 5). Hard titanium nitride coating has been deposited by physical vapor deposition (PVD) and chemical vapor deposition (CVD) techniques (Ref 6). However, due to the low deposition rate, the obtained TiN coatings are usually very thin (< 10 μm), which limits its application (Ref 7). Therefore, the reactive plasma spraying (R-PS) process is considered to manufacture thick TiN coatings (Ref 8, 9). For example, Xiao et al. made a more than 300-μm nanostructured TiN coating by R-PS. However, the layer contained Ti_3O except the main phase TiN, which affects the property of titanium nitride coating (Ref 8). VLPPS which is emerging Technology in the thermal spray community can improve these two major drawbacks.

Very low-pressure plasma spraying (VLPPS) is a very promising manufacturing coating process that differs from traditional spray technology. It is performed in a controlled atmosphere chamber at a lower pressure than traditional vacuum thermal spray processes (VPS and LPPS) leading to a new way to manufacture coatings (Ref 10). This process can offer a set of advantages (Ref 11-13):

- the plasma jet becomes increasingly longer and wider as the pressure decreases

🖄 Springer

- the lower density gradients between the plasma jet and the surroundings atmosphere result in more stable jets and less cold gas entrainment. As a result, better uniform particle heating and acceleration are got, with less divergence of the particles trajectories
- dense and defect-free coatings can be successfully manufactured with higher deposition rate than CVD, PVD
- the longer, wider and more stable jet permits to preheat the substrate to a desired temperature without oxidation of the substrate surface as with VPS/LPPS processes.

In view of the advantages of VLPPS, an in situ reaction may exist between the fed powder and the reactive gas injected on the surface of the substrate.

The purpose of this paper is to in situ synthesize titanium nitride coatings using the very low-pressure plasma spraying.

Materials and Methods

A pure titanium powder (99.99 at.%) whose size distribution is 7 to 23 μm (d_{50} = 13 μm) was used as feedstock for coating deposition. The powder is produced by Raymor AP&C (Boisbriand, QC, Canada).

A vacuum plasma spray system was employed to deposit coatings. A F4-VB torch (50 kW, Oerlikon–Metco, Switzerland) operated at a controlled atmosphere with very low pressure of 150 Pa. The detailed VLPPS operating parameters are listed in Table 1. At first, the chamber is pumped down to a pressure of 1 Pa, then filled with argon to 50 Pa and finally pumped down again to the desired operating pressure (150 Pa). The reactive gas nitrogen injected at the surface of the substrate with a pipe drilled with small holes (1 mm in diameter) localized just above the samples.

Stainless steel substrates were employed (25 mm in diameter) for the coating deposition. Before to spray, the substrates were grit-blasted with alumina grit to increase the bonding strength of the coating. The substrates were mounted on a horizontal bar as shown in Fig. 1. The plasma torch is moving up and down in front of the samples. The particles jet impacts for each pass on the substrate referenced "a." The other samples (b, c and d) are placed radically every 30 mm. A pyrometer is used to know the temperature on the sample "a."

To detect the light emissions of the evaporated titanium particles inside the plasma jet, an Optical Emission Spectroscope (OES) instrument (Jobin–Yvon spectrometer, TRIAX190, United Kingdom) equipped with a CCD detector was used. The properties are analyzed with the detector placed at 190 mm from the plasma jet axis. X-ray Diffraction (D8 Advance, Bruker AXS, Germany) was used to determine the compositions of the feedstock powder and VLPPS-sprayed coatings. Scan step was 0.02°/s with a step time of 1 s in the 20-80° 2θ range. Moreover, the mass fraction of phases was determined by Rietveld analysis which was conducted using JADE 6.0 software based on the spectrum through phase retrieval, pattern fitting and Rietveld refinement. A scanning electron microscope (FESEM JEOL 7800F, FEOL, Japan) was used to characterize the coating microstructure. Element composition was measured with EDS detector (SDDX-Flash 6130, Bruker, Germany). The relative density of the coating was estimated using image analysis (NIH Image J, Software, USA) of polished cross sections of the coating. A minimum of 10 continuous pictures (1000 ×) were analyzed for each sample.

The Vickers hardness (Miniload-2, Leitz, Germany) of coatings was measured on the polished cross section with a 300-g load and a dwell time of 15 s. Ten randomly located indentations were done.

Table 1 Parameters of the experiment

Parameters	Value
Pressure (Pa)	150
Plasma torch	F4-VB
Plasma forming gases (L min^{-1})	Ar/H$_2$ (45/12)
Reactive gas (L min^{-1})	N$_2$ (8)
Arc current intensity (A)	650
Voltage (V)	50
Carrier gas flow rate Ar (L min^{-1})	2.5
Spraying distance (mm)	900
Powder mass rate (g min^{-1})	2.5
Substrate temperature (°C)	800
sample a	

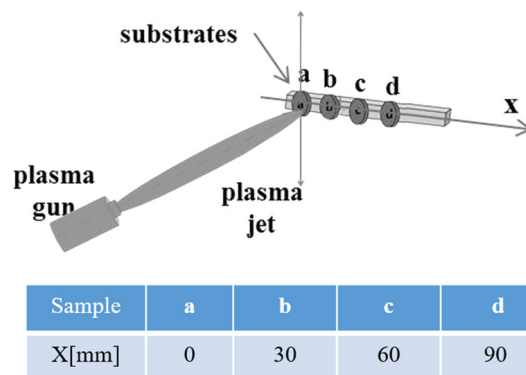| Sample	a	b	c	d
X[mm]	0	30	60	90

Fig. 1 VLPPS experimental configuration

Results and Discussion

Plasma Jet Analysis

In this experiment, OES analyses were performed to detect the plasma visible light emission of evaporated Ti particles and gases (H_2, Ar) in the wavelength range from 300 to 900 nm. Figure 2 shows the OES patterns of the plasma jet in the experiment determined for different radial distances from plasma jet axis (0, 30, 60 and 90 mm). Ar deals with red color, H_2 with black one and Ti with blue one.

It appears that Ti powder has been transformed into a vapor state. In addition, the emission intensity of the excited Ti ions and plasma gas elements (H_2, Ar) are gradually reduced with the increase in the radial distance from 0 to 90 mm. Because the energy exchange results from the collision between atoms and heavy particles in the plasma jet (Ref 14). Hence, the plasma density and temperature decreased with the radial distance because the plasma jet has a lower intensity with the expansion of plasma jet along the radial direction.

Coatings Microstructure

Figure 3 presents the coatings cross sections. As supposed and showed by the OES measurements, the thickness decreases along the radial distance from about 105 μm (coating (a)) to 38 μm (coating (d)). Because reactant concentration (Ti, N_2) gradually decreases as the radial distance decreases. Coatings are rather dense with a porosity ratio varied from 0.8 to 2% as radial distance increases. Figure 4 shows high resolution at high magnification of the resulting microstructures. All the coatings consist of a hybrid deposition of semi-molten particles, liquid splats, cluster and vapors with different fractions. For the coatings (a) and (b) (X axis = 0, 30 mm), the molten particles impact onto the substrate and spread as lamellae. In the same time, clusters and vapors adhere, diffuse and nucleate on the splat/substrate (Ref 15). On the high-temperature surface (800 °C for sample "a"), the injected reactive gas N_2 reacts with nucleated particles and lamellae to form titanium nitride phases. EDS analyses are shown in Fig. 5. It signifies that nitride phases already generated.

To increase furthermore the TiN phase, higher power is required for the torch. Because vapor mode is the best condition to improve the nitridation of titanium. During the deposition process, the nuclei of the vapors will grow as a columnar structure in theory. However, in this experiment owing to the high reactant concentration, the high proportion of particles in a melted phase induces lamellae formation at impact. The columnar growth is affected, and
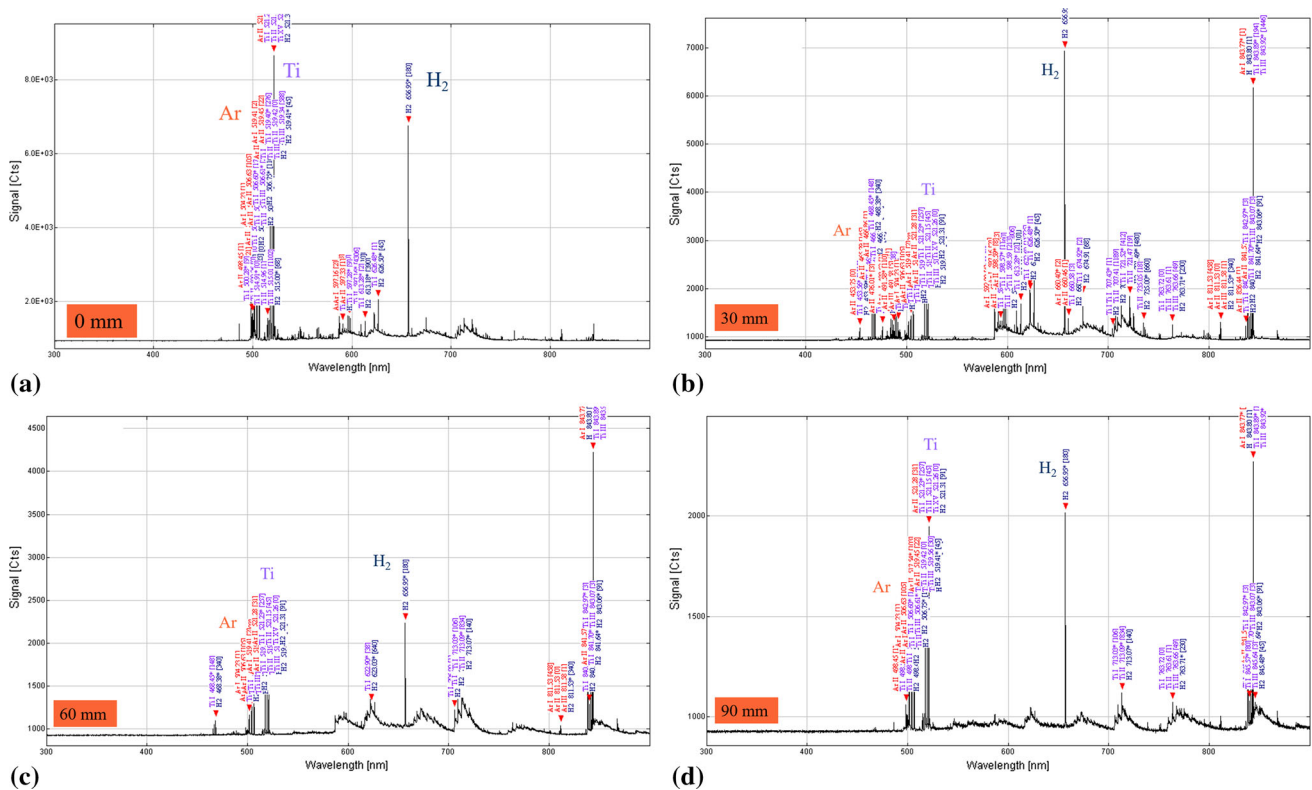

Fig. 2 OES patterns of the plasma jet with Ti powder for different radial distances (a) 0 mm, (b) 30 mm, (c) 60 mm, (d) 90 mm
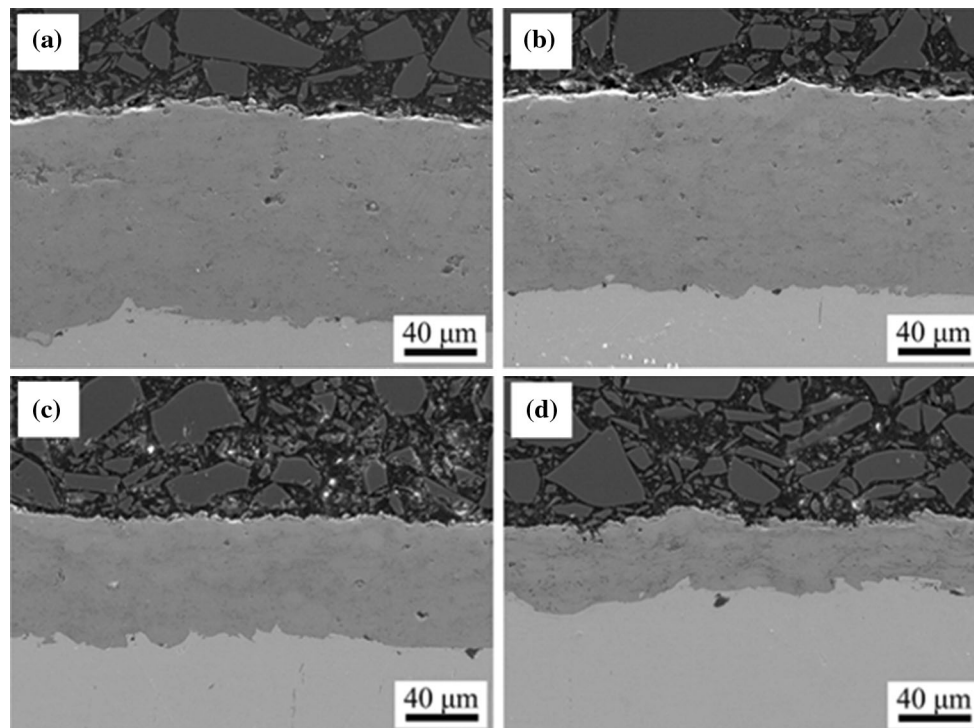
Fig. 3 Coatings cross section for different radial distances from plasma jet axis: (a) 0 mm, (b) 30 mm, (c) 60 mm and (d) 90 mm
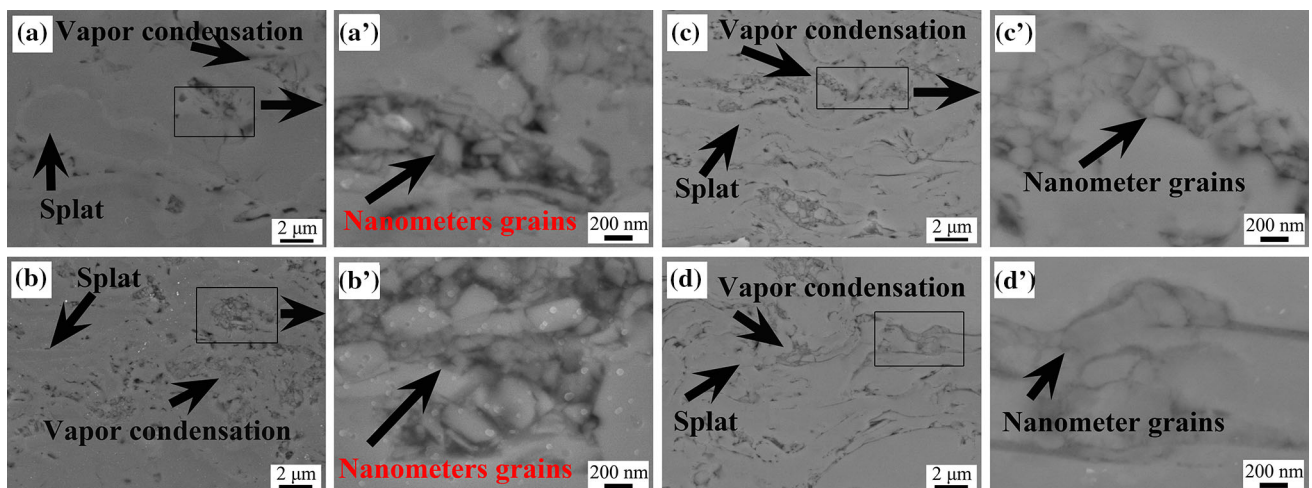

Fig. 4 High-magnification cross-sectional morphologies of the coatings for different radial distances from plasma jet axis: (a, a') 0 mm, (b, b') 30 mm, (c, c') 60 mm and (d, d') 90 mm

irregular nano-sized grains are obtained, as we can see in Fig. 4. Additively, the size of the grains in coating (d') is bigger than that of coatings (a'), (b') and (c'). This is because the temperature of the substrate is lower than the coatings located front of the plasma plume and the cooling rate is smaller. Also, the velocity of plasma jet is as high as 800 m/s, so the residence time of powders inside the plasma jet is less than 10^{-4} s (Ref 16). Thus, nano-sized grains have few times to grow up during plasma spray process, and finally are embedded in the coatings. After

that, the cooling velocity of the deposited coating can reach 10^6-10^7 K/s (Ref 17). Another explanation can be that close to the plasma jet axis, the temperature is higher resulting in better vaporization efficiency and a condensation on the substrate. If the radial distance increases, the condensation and the agglomeration of the particles could occur before impacting on the substrate, inducing bigger particles. As a result, the irregular grains with diameters ranging from several tens to hundreds of nanometers formed in the coatings.
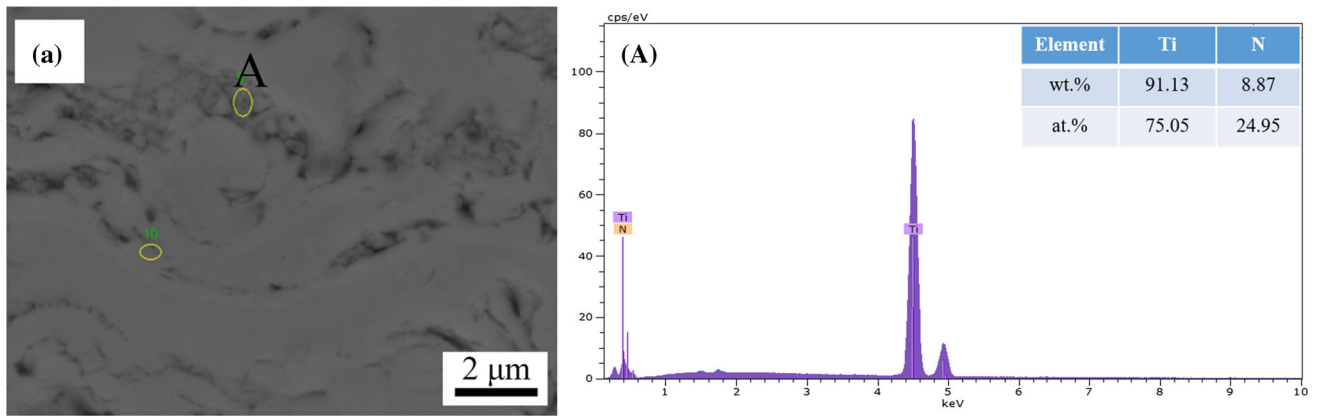
Element	Ti	N
wt.%	91.13	8.87
at.%	75.05	24.95

Fig. 5 EDS analyses of the cross-section of the coating (a) at the radial distance 0 mm

Nano-sized ball particles
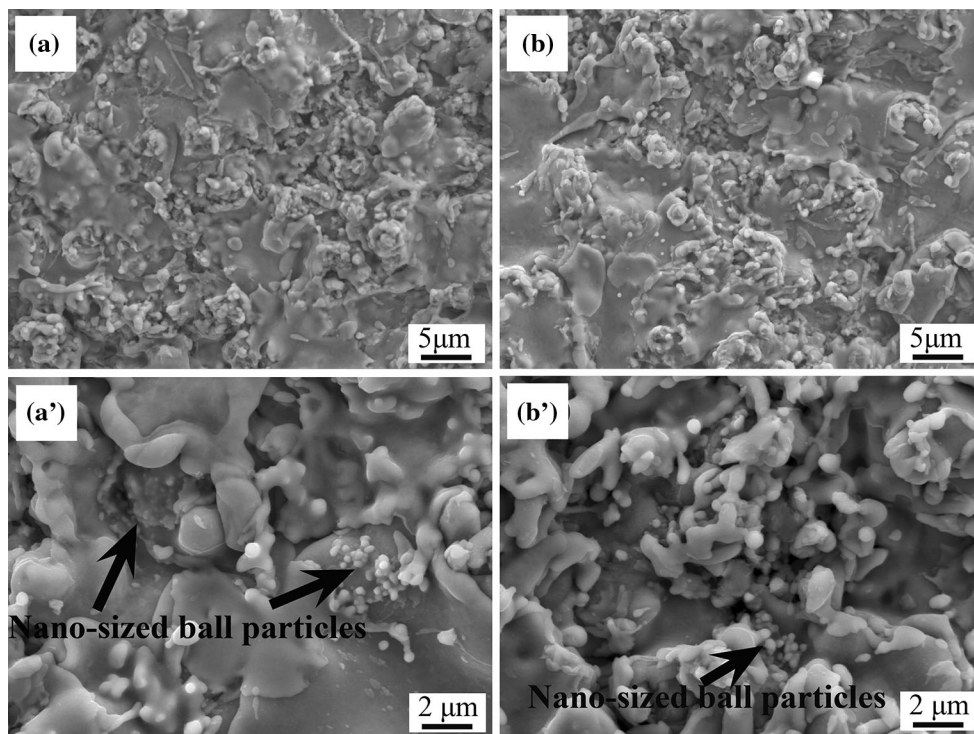
Nano-sized ball particles

Fig. 6 Surface morphology of the coatings for different radial distances from plasma jet axis: (a) 0 mm, (b) 30 mm

There are no apparent differences in surface morphologies. The coatings surface reveals splats with an average diameter ranging from 5 to 10 μm, spherical particles with diameters from 0.5 to 2 μm and some nanosized ball particles (Fig. 6). EDS analyses of the surface morphology of the coating are shown in Fig. 7. It exposes that nanometer particles are composed of higher nitride phase than lamellae.

Phase Composition and Micro-hardness

The XRD patterns of the resulting coatings are displayed in Fig. 8. The phases obtained include $TiN_{0.3}(\alpha-Ti(N))$ and Ti_2N, TiN without oxides or residual Ti, compared to other TiN coatings by made by R-PS (Ref 8, 9). In addition, the mass fraction of the phases is obtained by Rietveld analysis and is shown in Table 2. The mass fraction of the TiN phase gradually decreases with the radial distance from 56.6% (0 mm) to 7.9% (90 mm). The mass fraction of the $TiN_{0.3}$ phase increases with radial distance from 36.8% (0 mm) to
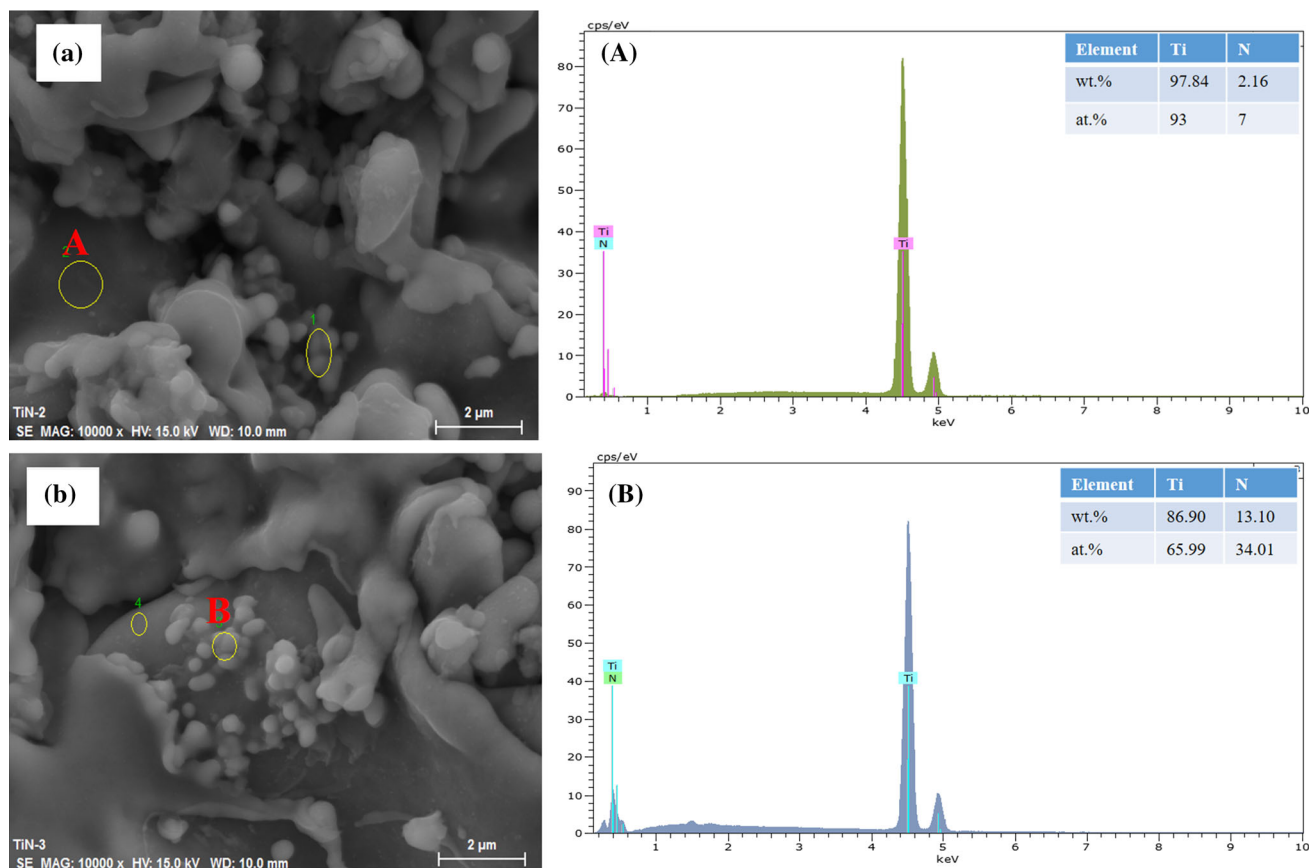
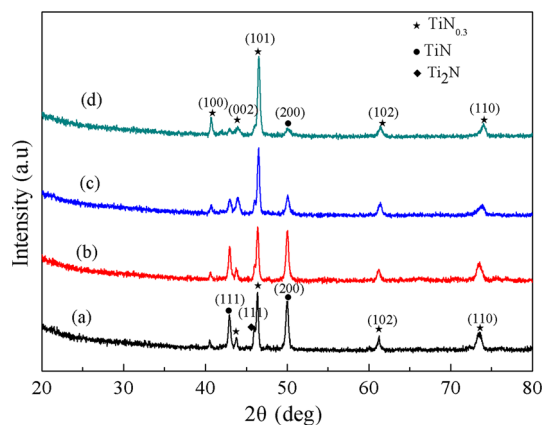**Fig. 7** EDS analyses of the coating for different radial distances from plasma jet axis: (a) 0 mm, (b) 30 mm

Fig. 8 XRD pattern of the coatings for different radial distances from plasma jet axis: (a) 0 mm, (b) 30 mm, (c) 60 mm and (d) 90 mm

92.1% (90 mm). These results indicate that the nitridation efficiency of Ti powder is relatively low; the nitridation efficiency gradually decreases as the radial distance increases. Because the low power of the torch restricted vaporization of Ti powder during the flight, the nitridation reaction on the substrate is limited. Therefore, even the coating located on the center of the plasma jet is with low nitridation efficiency (56.6%). Moreover, as the radial distance increases, the injected Ti particles flight into the low-temperature region of the plasma jet. Thermal transfers from plasma to injected powder are lower. So, the injected Ti powder could not be well melted or vaporized. Besides, the temperature of the substrate is relative lower than that of substrate located on the center of the plasma jet. So, the nitrogen and Ti powders react on the substrate with lower

Table 2 Mass fraction of phases at different radial distances

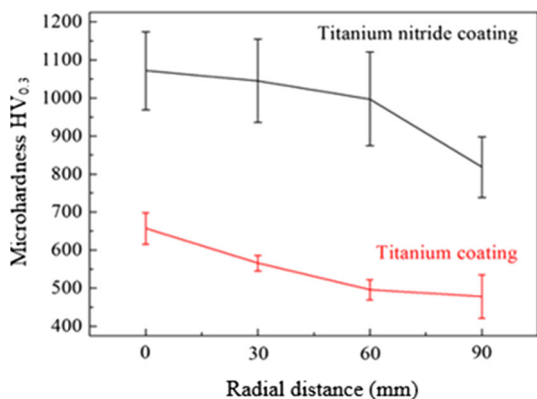| Radial distance (mm)	TiN phase (%)	Ti_2N phase (%)	$TiN_{0.3}$ (%)
0	56.6	19.3	24.2
30	47.7	15.4	36.8
60	32	10.2	57.9
90	7.9	0	92.1

Fig. 9 Vickers hardness of titanium nitride coatings for different radial distances from plasma jet axis (0, 30, 60 and 90 mm) compared to pure titanium one manufactured in the same conditions in a previous study

Fig. 10 Normalized nitride fractions (ATOT) vs. hardness

activation energy. As a result, the mass fraction of TiN generated is quite low with only 7.9%.

The Vickers hardness is shown in Fig. 9. The hardness of the coatings gradually decreases with increasing the radial distance. Front of the plasma jet, the highest value is obtained: 1071 $HV_{0.3}$. At 90 mm from the jet axis, the hardness is 250 $HV_{0.3}$ lower (817 $HV_{0.3}$). The relationship between nitridation ratio of the coating and its hardness was investigated by the calculation of nitride phases amount (Ti_2N, TiN) in coating. This was done by calculating the ratios, proportional to their volumetric fraction, with respect to the α-Ti(N), according to the following equation (Ref [18]):

$$a_{\text{TiN},i} = \frac{\text{height of the most significant TiN peak}}{\text{height of the most significant } \text{TiN}_{0.3} \text{ peak}}$$

$$a_{\text{Ti}_2\text{N},i} = \frac{\text{height of the most significant } \text{Ti}_2\text{N peak}}{\text{height of the most significant } \text{TiN}_{0.3} \text{ peak}}$$

where the index i refers to the sample numbers. Normalized factors, Ai, for both TiN and Ti_2N phases, were derived from the respective ai, according to the following equations:

$$A_{\text{TiN},i} = \frac{a_{\text{TiN},i}}{a_{\text{TiN}}^{\text{MAX}}}$$

$$A_{\text{Ti}_2\text{N},i} = \frac{a_{\text{Ti}_2\text{N},i}}{a_{\text{Ti}_2\text{N}}^{\text{MAX}}}$$

where $a_{\text{TiN}}^{\text{MAX}}$ and $a_{\text{Ti}_2\text{N}}^{\text{MAX}}$ are the maximum values obtained among all the samples. Furthermore, normalized factors $A_{\text{TOT},i}$ for both phases were defined for each sample as it follows:

$$A_{\text{TOT},i} = \frac{A_{\text{TiN},i} + A_{\text{Ti}_2\text{N},i}}{2}$$

The experimental results were in the range 0.04-1.00 for A_{TiN}, 0.34-1.0 for A_{Ti2N} and 0.49-1.0 for A_{TOT}, thus

confirming different amounts of nitride fractions at different radial distances of the plasma. In Fig. 10, the coating hardness (different radial distances) versus total amount of nitride fractions is shown. Figure 10 shows the hardness increased with augmenting nitride content and this behavior was almost linear. Because the amount of the nitride phases (Ti_2N, TiN) decreases as the radial distance increases. Hence, the hardness of the coatings (a) and (b) is higher than coatings (c) and (d). Compared to pure titanium coating manufactured in the same conditions in a previous study (Ref [19]), the injection of nitrogen at the substrate surface is efficient to create nitrides. Moreover, the hardness is higher than other TiN coatings manufactured by R-PS (Ref [9, 18]).

Conclusions

A VLPPS in situ reaction process for the synthesis of composite titanium nitride coating was successfully developed. A reactive gas (nitrogen) is injected on heat substrate surface (800 °C) to generate the reactions with feedstock Ti particles and as-deposits. The deposited coating was investigated at different radial distances of the plasma plume. There is no evident difference about the morphologies of the coating at different radial distances. All the coatings are deposited by the mixed lamellae of molten, clusters and vapors. Additively, the phases of the coatings are composed of nitrides TiN Ti_2N and some $TiN_{0.3}$ phases. When the radial distance increases, the mass fraction of the nitrides TiN Ti_2N peaks gradually reduces, on the contrary to $TiN_{0.3}$. The micro-hardness increased with augmenting nitride content, and this behavior was almost linear. The hardness of the coating is quite high especially in front of the plasma jet where TiN amount was higher (1071 $HV_{0.3}$). To increase furthermore TiN phase and so the hardness, a higher-power torch or the narrow powder size distribution could be applied to get higher vapor amount to improve the reaction with nitrogen.

References

1. A.P. Serro, C. Completo, R. Colaço, F. dos Santos, C. Lobato da Silva, J.M.S. Cabral, H. Araújo, E. Pires, and B. Saramago, A Comparative Study of Titanium Nitrides, TiN, TiNbN and TiCN, as Coatings for Biomedical Applications, *Surf. Coat. Technol.*, 2009, **203**, p 3701-3707

2. B. Subramanian, C.V. Muraleedharan, R. Ananthakumar, and M. Jayachandran, A Comparative Study of Titanium Nitride (TiN), Titanium Oxy Nitride (TiON) and Titanium Aluminum Nitride (TiAlN), as Surface Coatings for Bio Implants, *Surf. Coat. Technol.*, 2011, **205**, p 5014-5020

3. B. Tian, W. Yue, C. Wang, and J. Liu, A Comparative Study of Titanium Nitride (TiN), Titanium Oxy Nitride (TiON) and Titanium Aluminum Nitride (TiAlN), as Surface Coatings for Bio Implants, *Surf. Coat. Technol.*, 2011, **205**, p 5014-5020

4. A. Bahri, N. Guermazi, K. Elleuch, and M. Ürgen, Tribological Performance of TiN Coatings Deposited on 304L Stainless Steel Used for Olive-Oil Extraction, *Wear*, 2015, **342**, p 77-84

5. X. Shi, L. Xu, M. Munar, and K. Ishikawa, Hydrothermal Treatment for TiN as Abrasion Resistant Dental Implant Coating and Its Fibroblast Response, *Mater. Sci. Eng. C*, 2015, **49**, p 1-6

6. B. Elsener, A. Rota, and H. Böhni, Impedance Study on the Corrosion of PVD and CVD Titanium Nitride Coating, *Mater. Sci. Forum*, 1989, **44-45**, p 29-38

7. F. Lang and Z. Yu, The Corrosion Resistance and Wear Resistance of Thick TiN Coatings Deposited by Arc Ion Plating, *Surf. Coat. Technol.*, 2001, **145**(1-3), p 80-87

8. L. Xiao, D. Yan, J. He, L. Zhu, Y. Dong, J. Zhang, and X. Li, Nanostructured TiN Coating Prepared by Reactive Plasma Spraying in Atmosphere, *Appl. Surf. Sci.*, 2007, **253**(18), p 7535-7539

9. V. Serban, R. Rosu, A. Bucur, and D. Pascu, Deposition of Titanium Nitride Layers by Electric Arc-Reactive Plasma Spraying Method, *Appl. Surf. Sci.*, 2013, **265**, p 245-249

10. K. Niessen and M. Gindrat, Plasma Spray-PVD: A New Thermal Spray Process to Deposit Out of the Vapor Phase, *J. Therm. Spray Technol.*, 2011, **20**(4), p 736-743

11. M.F. Smith, A.C. Hall, J.D. Fleetwood, and P. Meyer, Very Low-Pressure Plasma Spray—A Review of an Emerging Technology in the Thermal Spray Community, *Coatings*, 2011, **1**(2), p 117-132

12. X. Fan, G. Darut, M. Planche, H. Liao, and G. Montavon, Formation Mechanisms of In-situ Al Based Intermetallic Coatings Manufactured by Very-Low Pressure Plasma Spraying, *Surf. Coat. Technol.*, 2018, **334**, p 300-304

13. L. Zhu, N. Zhang, B. Zhang, R. Bolot, and H. Liao, Synthesis and Microstructure Observation of Titanium Carbon Nitride Nanostructured Coatings Using Reactive Plasma Spraying in Atmosphere, *Appl. Surf. Sci.*, 2011, **257**, p 8722-8727

14. C. Pierlot, L. Pawlowski, M. Bigan, and P. Chagnon, Design of Experiments in Thermal Spraying: A Review, *Surf. Coat. Technol.*, 2008, **202**, p 4483-4490

15. X. Lin, Y. Zeng, X. Zhou, and C. Ding, Microstructure of Alumina-3wt.% Titania Coatings by Plasma Spraying with Nanostructured Powders, *Mater. Sci. Eng. A*, 2003, **357**, p 228-234

16. Y. Zhu, C. Deng, K. Yukimura, and T. Xiao, Deposition and Characterization of Nanostructured WC-Co Coating, *Ceram. Int.*, 2001, **27**, p 669-674

17. S. Cirolini, J.H. Harding, and G. Jacucci, Computer Simulation of Plasma Sprayed Coatings, *Surf. Coat. Technol.*, 1991, **48**(2), p 137-145

18. G.M. Ingo, S. Kaciulis, A. Mezzi, T. Valente, F. Casadei, and G. Gusmano, Characterization of Composite Titanium Nitride Coatings Prepared by Reactive Plasma Spraying, *Electrochem. Acta*, 2005, **50**(23), p 4531-4537

19. X. Fan et al, Characterization of Ti Coatings Deposited by Very Low-Pressure Plasma Spraying. In: Proc 8th RIPT2017, Limoges, France (2017)